ChemistrySelect, **4**, 5984-5987 (2019).

Charge and Discharge Reactions of a Lead Fluoride Electrode in a Liquid-Based Electrolyte for Fluoride Shuttle Batteries: -The Role of Triphenylborane as an Anion Acceptor-

Hiroaki Konishi,*[a] Taketoshi Minato,*[b] Takeshi Abe,*[c] and Zempachi Ogumi[a]

Abstract: Lead fluoride (PbF_2) is a promising electrode material for fluoride shuttle batteries (FSBs) owing to its high theoretical capacity (219 mAh g^{-1}). In this study, the discharge and charge capacities of a PbF_2 electrode were measured using a bis[2-(2-methoxyethoxy)ethyl] ether containing cesium fluoride and triphenylborane as an electrolyte. A high specific capacity was maintained during both the discharge and charge processes in the first cycle, but the capacity decreased from the first charge process to the following discharge process. To clarify the electrochemical reaction mechanism, the dissolution and change in the electronic state of Pb at the PbF_2 electrode during the discharge and charge processes were evaluated via atomic absorption spectrometry (AAS) and X-ray photoelectron spectroscopy (XPS). The results obtained from AAS and XPS indicated that Pb was formed during the discharge process. Conversely, the formation of PbF_2 and dissolution of Pb coexisted within the wide range of charge process. The PbF_2 could react in the following cycle, but the dissolved Pb was unable to contribute to the following discharge/charge reaction. Therefore, after the initial charge process, the capacity decreased.

To improve the performance of portable electronic devices, a range of batteries have been developed [1–11]. Recently, Reddy et al. proposed a battery based on fluoride ion migration [12], since then several research groups have further developed these batteries [13–15]. Our group has developed an organic-solvent-based electrolyte that contains supporting electrolyte salt and an anion acceptor (AA) for use in a fluoride shuttle battery (FSB) [16–19]. The development of organic-solvent-based electrolytes for FSBs was accomplished through the utilization of an AA, which supports the dissolution of insoluble inorganic fluoride compounds as a supporting electrolyte salt in an organic solvent. A metal fluoride (MF_x) is used as the active material for this type of battery. The electrochemical reaction of MF_x starts at the discharge process, during which the metal (M) is formed ($MF_x + xe^- \rightarrow M + xF^-$). Then, MF_x is formed ($M + xF^- \rightarrow MF_x + xe^-$) during the charge process.

Previously, the charge and discharge measurements for the bismuth fluoride (BiF_3) and lead fluoride (PbF_2) electrodes were conducted in an electrolyte comprising cesium fluoride (CsF), (fluorobis(2,4,6-trimethylphenyl)borane (FBTMPhB)), and (bis[2-(2-methoxyethoxy)ethyl] ether (tetraglyme: G4)) as the supporting electrolyte salt, AA, and an organic solvent. The discharge and charge reactions of the BiF_3 and PbF_2 electrodes progressed in this electrolyte. However, after one cycle, the shape of the discharge curve changed and the discharge capacity decreased greatly [16]. We previously found that triphenylborane (TPhB) and triphenylboroxine (TPhBX) could also be used as AAs [19]. Using the electrolytes containing TPhB/TPhBX, the charge and discharge measurements of BiF_3 electrode were conducted. The change in the shape of the discharge curve was suppressed when using these AAs. The cycling performance of the BiF_3 electrode was affected by the type of AA used. The cycling performance in the electrolyte with TPhB was higher than that with TPhBX [19].

In this study, the electrochemical properties of a PbF_2 electrode were investigated by using an electrolyte comprising CsF, TPhB, and G4. Here, we verified the ability of TPhB to act as an AA via the density functional theory (DFT) calculation. After the optimized molecular structure of TPhB was calculated, the most stable binding site of F^- on TPhB and its adsorption energy (*Ea*) were calculated. After confirming that TPhB behaves as an AA, the electrochemical measurements of the PbF_2 electrode were performed using an electrolyte with TPhB. PbF_2 mixed with carbon, by using a ball mill, was used as the active material because this method has been reported to improve the electrochemical properties of MF_x electrodes [20–25]. The electrochemical reaction mechanism of the PbF_2 electrode was investigated via atomic absorption spectrometry (AAS) and X-ray photoelectron spectroscopy (XPS).

[a] Dr. H. Konishi, Prof. Z. Ogumi
Office of Society-Academia Collaboration for Innovation
Kyoto University
Gokasho, Uji, Kyoto 611-0011, Japan
E-mail(H. Konishi): hiroaki.konishi.yj@hitachi.com
(Present address)
Dr. H. Konishi
Research & Development Group
Hitachi Ltd.
1-1, Omika-cho 7-chome, Hitachi, Ibaraki 319-1292, Japan
E-mail: hiroaki.konishi.yj@hitachi.com

[b] Prof. T. Minato
Office of Society-Academia Collaboration for Innovation
Kyoto University
Katsura, Nishikyo, Kyoto 615-8530, Japan
E-mail(T. Minato): minato.taketoshi.5x@kyoto-u.ac.jp

[c] Prof. T. Abe
Graduate School of Engineering
Kyoto University
E-mail(T. Abe): abe@elech.kuic.kyoto-u.ac.jp
Nishikyo-ku, Kyoto 615-8510, Japan

Supporting information for this article is given via a link at the end of the document.((Please delete this text if not appropriate))

ChemistrySelect, **4**, 5984-5987 (2019).

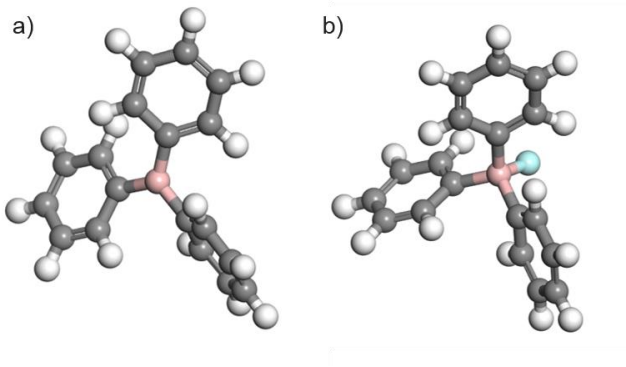

Figure 1. Structures of a) TPhB and b) TPhB–F^- after optimization. The gray, white, pink, and aqua balls represent carbon, hydrogen, boron, and fluorine, respectively.

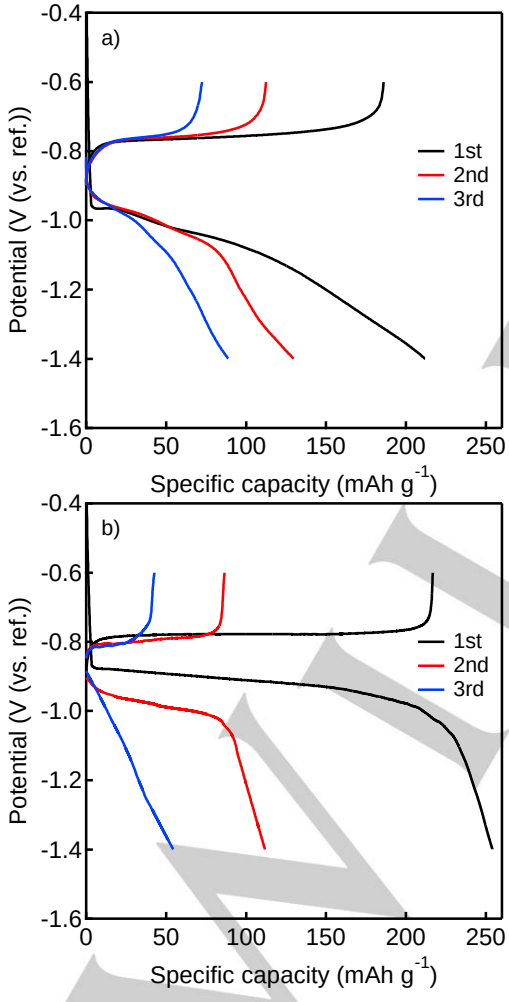

Figure 2. Discharge and charge curves for the PbF_2 electrode at a) 1/10 and b) 1/40 C over the potential range from –1.4 to –0.6 V (vs. ref.).

The ability of TPhB to act as an AA to coordinate with F^- was estimated from the *Ea* value of TPhB–F^- obtained from DFT calculations. The optimized molecular structure of TPhB obtained from the calculation is illustrated in Figure 1(a). The boron atom (shown as a pink ball in Figure 1(a)) is located at the center of the molecule and is coordinated with three phenyl rings (shown as gray and white balls in Figure 1(a)). The most stable binding site for F^- (shown as an aqua ball in Figure 1(b)) on TPhB was found to be the boron atom, as shown in Figure 1(b). The *Ea* of F^- on TPhB was –324.3 kJ mol^{-1}, which is similar to those of an efficient AA such as FBTMPhB or tris(pentafluorophenyl)borane [16, 26]. The calculation results indicate that TPhB is an appropriate molecule to act as an AA in an organic electrolyte.

Using G4 containing CsF and TPhB as a supporting electrolyte salt and AA, respectively, the charge and discharge measurements of the PbF_2 electrode were conducted at 1/10 and 1/40 C (Figure 2), respectively. When PbF_2 was cycled at 1/10 C (Figure 2(a)), the first, second, and third discharge/charge capacities were 212/186, 130/112, and 89/72 mAh g^{-1}, respectively. The first discharge capacity was close to the theoretical capacity (219 mAh g^{-1}); however, the capacity decreased in the following cycles. In order to progress the electrochemical reaction, the operating current condition was changed from 1/10 C to 1/40 C. At 1/40 C (Figure 2(b)), the first discharge capacity (254 mAh g^{-1}) was higher than the theoretical capacity. This suggests that the electrolyte might decompose during the first discharge process, which has observed in an LIB operated in an organic electrolyte [27–30]. Furthermore, the high capacity (217 mAh g^{-1}), which is close to the theoretical capacity, was obtained during the first charge process. However, the discharge/charge capacities then decreased as the cycle progressed. The change from 1/10 C to 1/40 C in the operating current condition decreased the polarization and increased the discharge/charge capacities. However, the capacity degradation during the cycle cannot be improved.

As reported previously, an electrolyte containing an AA can dissolve CsF and active material [16]. In this study, we assumed that the Pb is dissolved in the electrolyte during the charge process. To access the progress of Pb dissolution, the amount of Pb dissolved in the electrolyte during the charge process in the first cycle was measured. The results obtained through AAS indicate that 46% of the Pb is dissolved during the charge process in the first cycle, indicating that a charge capacity of 101 mAh g^{-1} is attributed to the dissolution of Pb ($Pb \rightarrow Pb^{2+} + 2e^-$). The dissolution of Pb causes a loss of active material; therefore, the capacity greatly decreases from the first charge to second discharge processes (Figure 2). However, the remainder of the charge capacity (116 mAh g^{-1}) may be attributed to the formation of PbF_2 ($Pb + 2F^- \rightarrow PbF_2 + 2e^-$).

The formation of PbF_2 during the charge process can be confirmed by the change in the electronic state of Pb in the electrode. Further, the progress of Pb formation in the discharge process might be clarified from the change in the electronic state of Pb in the electrode. The electronic states of Pb in the electrode during the discharge and charge processes were investigated through XPS (Figure 3). Two peaks, both assigned to Pb^{2+} (PbF_2), are observed at 139.0 and 143.9 eV in the pristine state (bottom in Figure 3) [31]. In addition to the peaks assigned to Pb^{2+} (PbF_2), peaks indexed to Pb metal were observed at 136.6 and 141.5 eV in the partially discharged state (100 mAh g^{-1}, second from bottom in Figure 3) [32]. There are two small peaks, indexed to Pb^{2+} (139.0 and 143.9 eV), and two large peaks, indexed to Pb metal (136.6 and 141.5 eV), in the fully discharged state (third from bottom in Figure 3). The changes in the peak intensities during the discharge process indicate that the amount of PbF_2 in the active material decreases, and the amount of Pb in the electrode increases as the discharge reaction progresses. This means that Pb is formed during the discharge process. Conversely, four peaks, assigned to Pb^{2+} and Pb metal, were observed in the partially charged state (100 mAh g^{-1}, fourth from bottom in Figure 3). Two large peaks, indexed to Pb^{2+}, and two small peaks, indexed to Pb metal, were observed in the fully charged state (top in Figure 3). The changes in the peak intensities during the charge process indicate that the amounts of Pb^{2+} and Pb metal increase and decrease, respectively, as the charge reaction progresses.

ChemistrySelect, **4**, 5984-5987 (2019).

These intensity changes were observed at both 0–100 and 100–217 mAh g^{-1}, indicating that the formation of PbF_2 ($Pb + 2F^- \rightarrow PbF_2 + 2e^-$) progresses during both the initial to intermediate stages and intermediate to final stages of the charge process.

The experimental results indicate that the electrochemical reaction of PbF_2 in the electrolyte containing TPhB proceeds as follows:

In the discharge process, the Pb is formed according to the following formula:

$$PbF_2 + 2e^- \rightarrow Pb + 2F^- \quad (i)$$

In the charge process, the formation of PbF_2 and dissolution of Pb proceed according to the following formulae:

$$Pb + 2F^- \rightarrow PbF_2 + 2e^- \quad (ii)$$

$$Pb \rightarrow Pb^{2+} + 2e^- \quad (iii)$$

From the results obtained through the electrochemical and AAS measurements, the capacities of 116 and 101 mAh g^{-1} were attributed to the progress of reactions (ii) and (iii), respectively. According to Figure 2(b), only one plateau was observed in the first charge curve. This implies that reactions (ii) and (iii) proceed at the same/similar potential range. Furthermore, the XPS results (Figure 3) indicate that two types of reaction coexist within the wide range during the charge process.

The formed PbF_2 can contribute to the subsequent discharge/charge reactions but the dissolved Pb cannot. Since two types of reaction progress at the same/similar potential, it is difficult to simultaneously suppress the dissolution of Pb and improve the cycling performance by limiting the charge cut-off potential.

Currently, to suppress the Pb dissolution during the charge process, the effects of the AA type and CsF/AA ratio in the electrolyte on the electrochemical performance are being investigated. Furthermore, the electrochemical reaction mechanisms at the PbF_2 electrode in various electrolytes are being investigated through several analysis methods. The results of these methods will be reported in the near future.

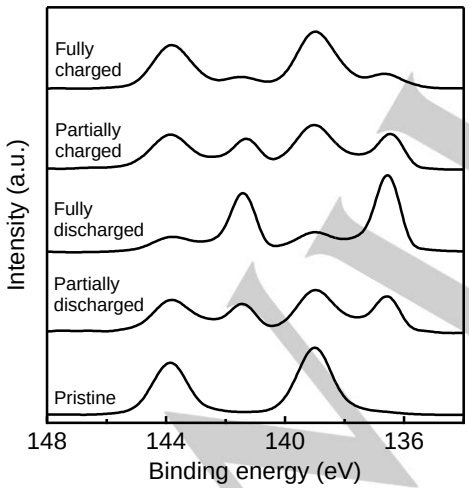

Figure 3. Pb 4f XPS spectra for the PbF_2 electrode in the pristine, partially discharged (100 mAh g^{-1}), fully discharged, partially charged (100 mAh g^{-1}), and fully charged states during the first cycle.

Supporting Information Summary

Information about the calculation method and experimental section is provided in the Supporting Information.

Acknowledgements

This work was supported by the Research and Development Initiative for Scientific Innovation of New Generation Batteries (RISING) and Research and Development Initiative for Scientific Innovation of New Generation Batteries 2 (RISING2) projects from the New Energy and Industrial Technology Development Organization (NEDO), Japan. Computation time was provided by the SuperComputer System, Institute for Chemical Research, Kyoto University. The authors thank Ms. Kiyomi Ishizawa, Ms. Ryoko Masuda, and Ms. Hisayo Ikeda for their experimental support.

Keywords: Anion acceptor • Fluoride shuttle battery • Lead fluoride • Triphenylborane

[1] B. Scrosati, J. Garche, *J. Power Sources* **2010**, *195*, 2419–2430.
[2] D. Miranda, C.M. Costa, S. Lanceros-Mendez, *J. Electroanal. Chem.* **2015**, *739*, 97–110.
[3] T. Minato, T. Abe, *Prog. Surf. Sci.* **2017**, *92*, 240–280.
[4] D. Capsoni, M. Bini, S. Ferrari, E. Quartarone, P. Mustarelli, *J. Power Sources* **2012**, *230*, 253–263.
[5] J. Lu, K.C. Lau, Y.K. Sun, L.A. Curtiss, K. Amine, *J. Electrochem. Soc.* **2015**, *162*, A2439–A2446.
[6] X. Li, J. Huang, A. Faghri, *J. Power Sources* **2016**, *332*, 420–446.
[7] M. Barghamadi, A. Kapoor, C. Wen, *J. Electrochem. Soc.* **2013**, *160*, A1256–A1263.
[8] J. Liu, Q. Zhang, Y.K. Sun, *J. Power Sources* **2018**, *396*, 19–32.
[9] M.I. Jamesh, A.S. Prakash *J. Power Sources* **2018**, *378*, 268–300.
[10] A. Eftekhari, D.W. Kim, *J. Power Sources* **2018**, *395*, 336–348.
[11] A.Parasuraman, T.M. Lim, C. Menictas, M. Skyllas-Kazacos, *Electrochim. Acta* **2013**, *101*, 27–40.
[12] M. A. Reddy, M. Fichtner, *J. Mater. Chem.* **2011**, *21*, 17059–17062.
[13] I. Mohammad, R. Witter, M. Fichtner, M.A. Reddy, *ACS Appl. Energy Mater.* **2018**, *1*, 4766–4775.
[14] M.A. Nowroozi, B. Laune, O. Clemens, *Chemistry Open* **2018**, *7*, 617–623.
[15] V.K. Davis, C.M. Bates, K. Omichi, B.M. Savoie, N. Momcilovic, Q. Xu, W.J. Wolf, M.A. Webb, K.J. Billings, N.H. Chou, S. Alayoglu, R.K. McKenney, I.M. Darolles, N.G. Nair, A. Hightower, D. Rosenberg, M. Ahmed, C.J. Brooks, T.F. Miller III, R.H. Grubbs, S.C. Jones, *Science* **2018**, *362*, 1144–1148.
[16] H. Konishi, T. Minato, T. Abe, Z. Ogumi, *J. Electrochem. Soc.* **2017**, *164*, A3702–A3708.
[17] H. Konishi, T. Minato, T. Abe, Z. Ogumi, *J. Appl. Electrochem.* **2018**, *48*,1205–1211.
[18] H. Konishi, T. Minato, T. Abe, Z. Ogumi, *J. Electroanal. Chem.* **2018**, *826*, 60–64.
[19] H. Konishi, T. Minato, T. Abe, Z. Ogumi, *Chem. Lett.* **2018**, *806*, 82–87.
[20] F. Badway, N. Pereira, F. Cosandey, G.G. Amatucci, *J. Electrochem. Soc.* **2003**, *150*, A1209–A1218.
[21] Y.L. Shi, M.F. Shen, S.D. Xu, Q.C. Zhuang, L. Jiang, Y.H. Qiang, *Solid State Ionics* **2012**, *222–223*, 23–30.
[22] H.J. Tan, H.L. Smith, L. Kim, T.K. Harding, S.C. Jones, B. Fultz, *J. Electrochem. Soc.* **2014**, *161*, A445–A449.
[23] H. Konishi, T. Minato, T. Abe, Z. Ogumi, *Chemistry Select* **2017**, *2*, 3504–3510.
[24] H. Konishi, T. Minato, T. Abe, Z. Ogumi, *Chemistry Select* **2017**, *2*, 6399–6406.
[25] H. Konishi, T. Minato, T. Abe, Z. Ogumi, *J. Electroanal. Chem.* **2017**, *806*, 82–87.
[26] Z. Chen, K. Amine, *J. Electrochem. Soc.* **2009**, *156*, A672–A676.
[27] E. Peled, *J. Electrochem. Soc.* **1979**, *126*, 2047–2051.
[28] E. Peled, D. Golodnitsky, G. Ardel, V. Eshkenazy, *Electrochim. Acta* **1995**, *40*, 2197–2204.
[29] V.A. Agubra, J.W. Fergus, *J. Power Sources* **2014**, *268*, 153–162.
[30] F. Badway, N. Pereira, F. Cosandey, G.G. Amatucci, *J. Electrochem. Soc.* **2003**, *150*, A1209–A1218.
[31] B. Huang, J.M. Hong, X.T. Chen, Z.L. Xue, X.Z. You, *J. Crystal Growth* **2005**, *276*, 491–497.
[32] H. Li, G. Zhang, L. Wang, *Wear* **2016**, *350–351*, 1–9.
[33] B. Delley, *J.Chem. Phys.* **1990**, *92*, 508–516.
[34] B. Delley, *J.Chem. Phys.* **2000**, *113*, 7756–7764.
[35] A.D. Becke, *J. Chem. Phys.* **1993**, *98*, 5648–5652.
[36] V. V. Pavlishchuk, A. W. Addison, *Inorg. Chim. Acta* **2000**, *298*, 97–102.

ChemistrySelect, **4**, 5984-5987 (2019).

ChemistrySelect, **4**, 5984-5987 (2019).

Entry for the Table of Contents

Insert graphic for Table of Contents here. ((Please ensure your graphic is in **one** of following formats))

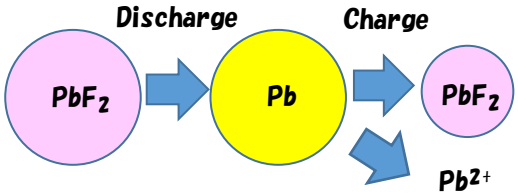

Electrochemical measurement of PbF_2 electrode for fluoride shuttle battery was performed in an electrolyte comprising G4, CsF, and TPhB. Initial discharge/charge capacities were high, but capacities were decreased in the following cycle. Analysis results indicate that Pb was formed during discharging, but PbF_2 formation and Pb dissolution coexisted during charging. The capacity degradation was caused by lack of active material due to Pb dissolution.